PLOS ONE

RESEARCH ARTICLE

Mapping quantitative trait loci and predicting candidate genes for leaf angle in maize

Ning Zhang, Xueqing Huang*

State Key Laboratory of Genetic Engineering, School of Life Sciences, Fudan University, Shanghai, China

* xueqinghuang@fudan.edu.cn

OPEN ACCESS

Citation: Zhang N, Huang X (2021) Mapping quantitative trait loci and predicting candidate genes for leaf angle in maize. PLoS ONE 16(1): e0245129. https://doi.org/10.1371/journal.pone.0245129

Editor: Maoteng Li, Huazhong University of Science and Technology, CHINA

Received: August 25, 2020

Accepted: December 22, 2020

Published: January 6, 2021

Peer Review History: PLOS recognizes the benefits of transparency in the peer review process; therefore, we enable the publication of all of the content of peer review and author responses alongside final, published articles. The editorial history of this article is available here: https://doi.org/10.1371/journal.pone.0245129

Data Availability Statement: All relevant data are within the paper and its Supporting Information files.

Funding: This work was funded by National Natural Science Foundation of China (grant number

Abstract

Leaf angle of maize is a fundamental determinant of plant architecture and an important trait influencing photosynthetic efficiency and crop yields. To broaden our understanding of the genetic mechanisms of leaf angle formation, we constructed a $F_{3:4}$ recombinant inbred lines (RIL) population to map QTL for leaf angle. The RIL was derived from a cross between a model inbred line (B73) with expanded leaf architecture and an elite inbred line (Zheng58) with compact leaf architecture. A sum of eight QTL were detected on chromosome 1, 2, 3, 4 and 8. Single QTL explained 4.3 to 14.2% of the leaf angle variance. Additionally, some important QTL were confirmed through a heterogeneous inbred family (HIF) approach. Furthermore, twenty-four candidate genes for leaf angle were predicted through whole-genome re-sequencing and expression analysis in qLA02-01and qLA08-01 regions. These results will be helpful to elucidate the genetic mechanism of leaf angle formation in maize and benefit to clone the favorable allele for leaf angle. Besides, this will be helpful to develop the novel maize varieties with ideal plant architecture through marker-assisted selection.

Introduction

Maize (Zea mays L.) is one of the most important cereal crops worldwide, and increasing the grain yield has been the most important goals of maize production [1]. Among the various traits that are normally considered in maize breeding programs, the leaf angle (LA), defined as the angle of leaf bending away from the main stem, is an important trait influencing plant architecture and yield production [2,3]. The less of leaf angle is, the more upright the leaves are. Upright leaves can maximize photosynthesis efficiency through maintaining light capture and reducing shading as canopies went more crowded, which in turn increase yield production in high density cultivation [3–6]. Therefore, an appropriate leaf angle is a prerequisite for attaining the desired grain yield in maize-breeding projects. A more thorough understanding of the molecular and genetic mechanism determining leaf angle will contribute to develop novel maize varieties with ideal plant architecture.

Genetic studies have indicated that leaf angle in maize is a complex trait controlled by both qualitative genes and quantitative genes. According to an incomplete statistic, eleven representative maize genes that control the leaf angle have been cloned, five of which were identified by mutagenesis: *knox* [7], *liguleless1* (*lg1*) [8], *liguleless2* (*lg2*) [9], *liguleless3* (*lg3*) [10], *liguleless narrow* (*lgn*) [11], and six were resolved through QTL-cloning approach: *ZmTAC1* [12],

31471151). The funder had no role in study design, data collection and analysis, decision to publish, or preparation of the manuscript.

Competing interests: The authors have declared that no competing interests exist.

ZmCLA4 [13], *ZmILI1* [14], and *UPA2/UPA1* [15], *ZmIBH1-1* [16]. In the past 30 years, a large number of QTL for leaf angle have been obtained by genetic dissection of maize leaf angle using biparental populations [17–24]. Mickelson et al. firstly identified nine leaf angle QTL which were distributed on six chromosomes in two environments using the RFLP marker technique in the B73 × Mo17 population containing 180 RILs [17]. Utilizing 1.49×10^6 single nucleotide polymorphism (SNP) markers, Lu et al. identified 22 SNP that were significantly associated with leaf angle and located on eight chromosomes, explaining 21.62% of the phenotypic variation [25]. The natural variations in leaf architecture were also discovered in connected RIL populations in maize. Tian et al. used nested association mapping (NAM) population from 25 crosses between diverse inbred lines and B73 to conduct joint linkage mapping for the leaf architecture, and identified thirty small-effect QTL for leaf angle [26]. A total of 14 leaf angle QTL were also identified using a four-way cross mapping population [27]. The large numbers of QTL for leaf angle detected in various mapping populations strengthen the understanding of the genetic mechanism of leaf angle in maize. However, different results were provided by different studies, including QTL number, location, and genetic effect. Inconsistent results of QTL detection in different study shown the importance and necessity of QTL mapping to uncover the tangled genetic mechanism of leaf angle. Therefore, taking the polygenic and complex inheritance nature of maize's leaf angle into consideration, further investigating the QTL that underlie the trait's phenotypic variance is required.

In the present study, a $F_{3:4}$ RIL population derived from a cross between inbred line B73 and Zheng58, was constructed to identify QTL for leaf angle. The objective of the study is to further elucidate the genetic architecture that underlie leaf angle, and to further evaluate and confirm the genetic effect of QTL allele through heterogeneous inbred family approach. It is expected that the further study into the genetic mechanism that underlies the leaf angle could provide candidate genes for maize breeding projects.

Materials and methods

Plant materials

The recombination inbred line population was constructed by crossing Zheng58 with B73. The two parents were selected on the basis of maize germplasm groups and their different leaf architecture. Zheng58 is an elite foundation inbred line with compact leaf architecture, as female parent of a famous maize variety Zhengdan958 in China. B73 is a model inbred line with expanded leaf architecture and has been sequenced [28]. A single seed descent from one F_1 progeny and then two generations of self-pollination were applied to produce the recombination inbred line population with 165 lines [29].

Field experiments and statistical analyses

The trials were conducted at the Songjiang experimental station in Shanghai (121˚45′E, 31˚12′N) from April to September during 2014 and 2015, where experimental field bases have been set up by the school of life sciences, Fudan University. More than two hundred lines were planted and 165 lines were survival. The school of life sciences was approved for field experiments, and the field studies did not involve protected or endangered species. The randomized complete block design with two replications was employed. Every plot had a row of three meters long and 0.67 meters wide with a planting density of 50,000 plants per hectare. Corn field management was in accordance with traditional Chinese agricultural production management methods.

Ten days after pollination (DAP), three plant representatives from the middle of each plot were randomly selected to evaluate the leaf angle. We measured three leaves and used the

mean value for data analysis. Traditionally, leaf angle was assessed by measuring the angle of each leaf from a plane defined by the stalk below the node subtending the leaf. Three consecutive leaves were measured for each plant, including the first leaf above the primary ear, the primary ear leaf and the first leaf below the primary ear. The leaf angle data for each of RIL populations was averaged for the three measured plants.

To further verify the authenticity of the QTL mapping results and the allelic effects of the leaf angle QTL, we constructed six heterogeneous inbred family (HIF) lines [30] from F_3 RIL segregating for target leaf angle locus but homozygous for the other major leaf angle loci. Each heterogeneous inbred family consisted of at least 120 plants and each individual from the progeny of these heterogeneous inbred family was genotyped using a molecular marker. And the molecular markers were tightly linked to the target QTL. Meanwhile, the leaf angle phenotype as described above was measured. ANOVA was used to compare and analyze phenotypic differences between different homozygous lines isolated in the target QTL region.

Statistical analysis of the phenotypic mean data measured in the population was performed using SPSS 20.0 software. The broad-sense heritability (h^2) was estimated as the proportion of variance explained by between RIL (genotypic) variance and RIL by block (error) variance.

Genetic map construction and QTL mapping

Samples for DNA extraction were collected at the four-leaf stage of the seedlings in the RIL population and parent line, and genomic DNA was isolated using the CTAB method [31]. The F_3 plants were genotyped using SSR markers. Primer sequences are available from the Maize Genetics and Genomic Database (Maize GDB).

The software package MapQTL6.0 was used to identify and locate QTL on the linkage map by using interval mapping and multiple-QTL model (MQM) mapping methods as described by Churchill et al. [32] and Huang et al. [33]. LOD threshold values applied to declare the presence of QTL were estimated by performing permutation tests implemented in Map QTL 6.0 using at least 1000 permutations of the original data set, resulting in a 95% log 10 of the odds ratio threshold values of 2.9. Using MQM mapping, the percentage of variance explained and the estimated additive genetic effect by each QTL and the total variance explained by all the QTL affecting a trait were obtained [33].

DNA library construction and Whole-genome re-sequencing analysis of Zheng 58

Extraction of total genomic DNA from young leaves of inbred line Zheng 58 by modified CTAB method [31]. Separation of genomic DNA used to generate sequencing libraries. The constructed library was first subjected to library quality checks, and the quality qualified library was sequenced by HiSeq system using standard protocols.

The raw readings (double-ended sequences) obtained by sequencing were quality assessed and filtered to obtain Clean Reads for subsequent bioinformatics analysis. The Burrows-Wheeler Alignment (BWA) software aligns the short sequences obtained from the second-generation high-throughput sequencing with the reference genome. The Clean Reads were compared with the reference genome sequence. The SNP and Small InDel were detected and annotated according to the comparison results.

Total RNA extraction and expression analysis of candidate genes

Fresh leaves in V5 stage were sampled from the B73 and Zheng58 [15]. According to the manufacturer's instructions, total RNA was isolated from sampled fresh leaves using Fast Pure Plant Total RNA Isolation Kit (Vazyme, RC401). 1.0 μg of each sample total RNA was reverse

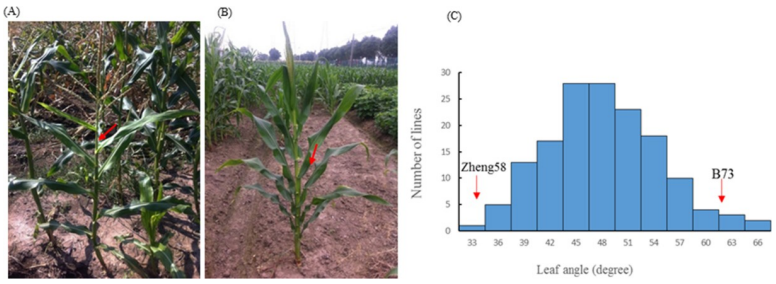

Fig 1. The maize leaf angle trait. (A) Leaf angle phenotype of the expanded inbred line B73. (B) Leaf angle phenotype of the compact inbred line Zheng58. (C) The frequency distribution of leaf angle within the $F_{3:4}$ population. The red arrow refers to the mean value of the leaf angle phenotype of the compact inbred line Zheng 58 and the expanded inbred line B73.

https://doi.org/10.1371/journal.pone.0245129.g001

transcribed (Vazyme, R323), and then performed Quantitative PCR (Vazyme, Q711). 18S was selected as housekeeping genes for the internal control, and the primers used in the RT-qPCR are listed in S1 Table. Three independent biological replicates were collected for each sample. The candidate genes expression levels were quantified with the comparative CT($2^{-\triangle\triangle CT}$) method.

Results and discussions

Analysis of leaf angle in $F_{3:4}$ population and parental lines

There was significant difference in leaf angle between the two parents B73 and Zheng58. Zheng58 had compact leaf architecture (Fig 1A) with an average leaf angle of 31˚, whereas B73 displayed expanded leaf architecture (Fig 1B) with an average leaf angle of 62˚ (Table 1). Table 1 presented the descriptive statistics of leaf angle for the two parents and the $F_{3:4}$ population. The wider range of variation for leaf angle in the $F_{3:4}$ population was observed, and normal distribution with transgressive segregation suggested polygenic inheritance of the trait (Fig 1C). The calculated broad-sense heritability (h^2) value for leaf angle trait was high as shown in Table 1.

Detection of the leaf angle QTL

189 SSR markers with polymorphic between the two parents were identified by the screen of 393 SSR primer pairs which evenly distributed on the genome of maize genome. These markers were assigned to corresponding chromosome based on their physical position. The total length of the physical map was 2,058.59 Mb. The number of molecular markers distributed on each chromosome varied from 13 to 29, with an average of 18.8. The average physical distance between two adjacent markers was 10.79 Mb, with the shortest marker interval of 1.42 Mb and the longest 38.78 Mb, and the distribution of all markers in chromosome was not crowded and relatively evenly distributed (Fig 2).

Table 1. Descriptive statistical analysis of phenotypic values of leaf angle in parents and $F_{3:4}$ population.

Trait	B73[a]	Zheng58[a]	$F_{3:4}$ population						
			Max	Min	Mean	SD	Kurtosis	Skewness	h^2 (%)
[b]LA	62.78	31.23	76.00	32.00	49.81	6.81	0.87	0.42	80.20

[a]The data corresponding to leaf angle of the two parents are average values; $P < 0.01$.

[b]LA: leaf angle.

https://doi.org/10.1371/journal.pone.0245129.t001

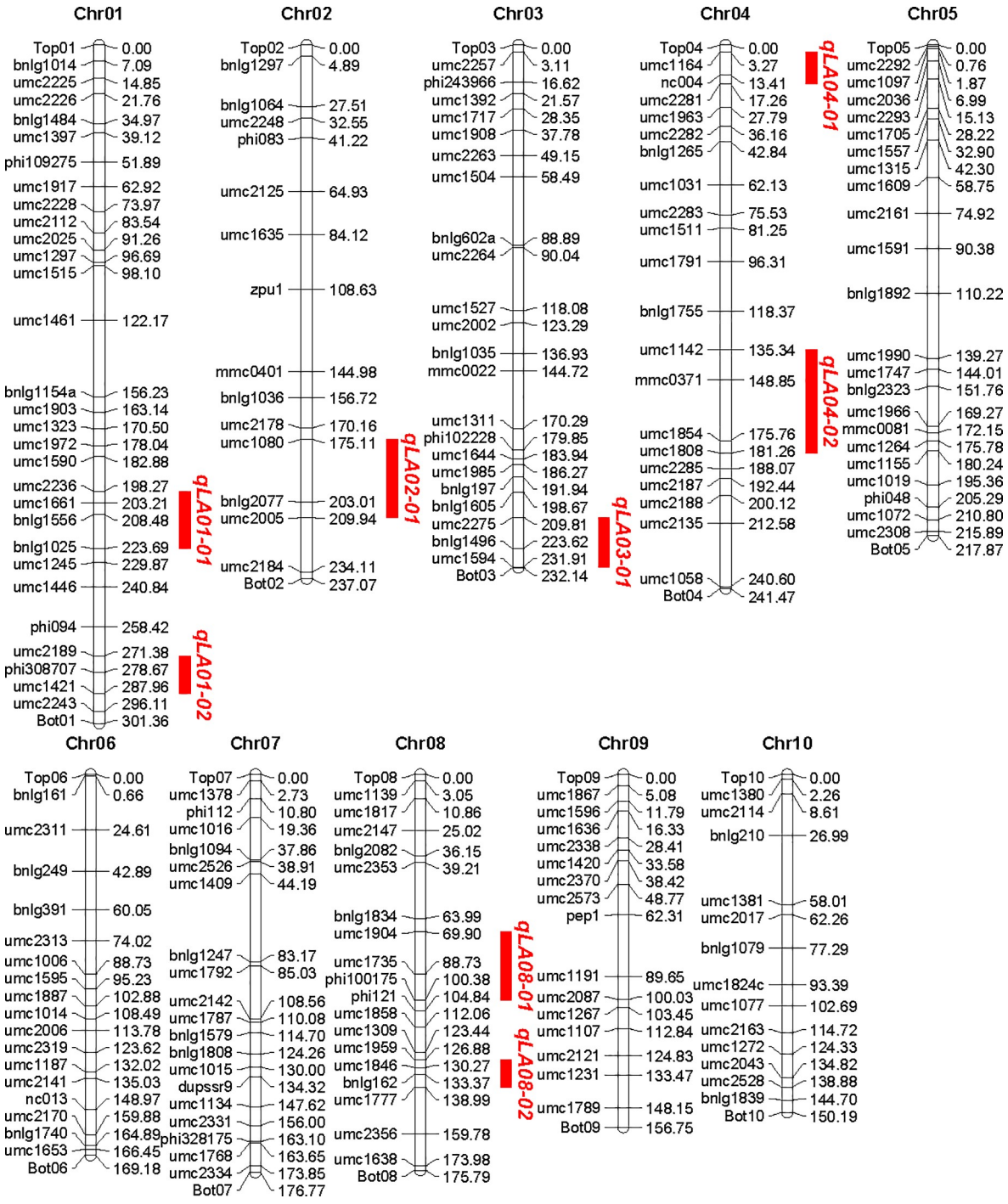

Fig 2. Construction of genetic linkage maps and mapping of QTL for controlling leaf angle in Maize.

https://doi.org/10.1371/journal.pone.0245129.g002

QTL analysis of leaf angle was conducted using Map QTL 6.0 software. Eight QTL for leaf angle on chromosome 1, 1, 2, 3, 4, 4, 8 and 8 were detected (Fig 2), respectively, which explained 65.4% of the total phenotypic variance, and each QTL explained phenotypic variance ranging from 4.3 to 14.2% (Table 2). It was noteworthy that all QTL had positive additive effects, suggesting that the B73 parent contributed most alleles for increasing leaf angle (Table 2).

Table 2. Analysis of QTL for controlling leaf angle.

QTL	Chr.	Position (Mb)	Marker interval	The nearest markers to QTL	LOD	Additive effect	Explained variance %
qLA01-01	1	211.78	umc2236-bnlg1025	bnlg1556	4.73	3.253	8.8
qLA01-02	1	285.67	umc2189-umc2243	umc1421	2.96	2.677	4.3
qLA02-01	2	195.48	umc1080-umc2005	bnlg2077	7.55	4.109	14.2
qLA03-01	3	220.49	umc2275-umc1594	bnlg1496	3.16	2.803	5.8
qLA04-01	4	10.68	umc1164-umc2281	nc004	4.95	3.445	9.1
qLA04-02	4	156.88	umc1142-umc1808	umc0371	3.67	3.082	6.7
qLA08-01	8	85.88	umc1904-phi100175	umc1735	5.2	3.687	10.3
qLA08-02	8	132.72	umc1959-umc1777	bnlg162	3.24	2.946	6.2

Additive effect: A positive value indicates that the B73 allele increases the value of the trait; A negative value indicates that the Zheng58 allele increases the value of the trait.

https://doi.org/10.1371/journal.pone.0245129.t002

Compared to previous studies (Fig 3), five of the eight QTL for leaf angle were found to have similar chromosomal locations with different mapping experiments or different genetic background. The result demonstrated that the chromosome regions for these consistent QTL might be hot spots for the important QTL for leaf angle. Also the congruence in QTL detected in this study with previous reports indicated the robustness of our results. However, in our study, no QTL was detected on chromosome 5, 6, 7, 9 and 10, which may be due to the too small genetic effects or no allelic difference between the two parents. Interestingly, three QTL were detected on bottom of chromosome 3 (qLA03-01), which shared an interval of 22.10 Mb from 209.81 to 231.91 Mb, middle of chromosome 4 (qLA04-02), which shared an interval of 45.92 Mb from 135.34 to 181.26 Mb, and middle of chromosome 8 (qLA08-01), which shared an interval of 30.48 Mb from 69.90 to 100.38 Mb, respectively. These three QTL have not been reported in previous researchers (Figs 2 and 3). These novel QTL might be due to the specific genetic background from parent Zheng58 with compact leaf architecture. Furthermore, newly detected major QTL may serve a complementary role in revealing the genetic mechanism of leaf angle trait.

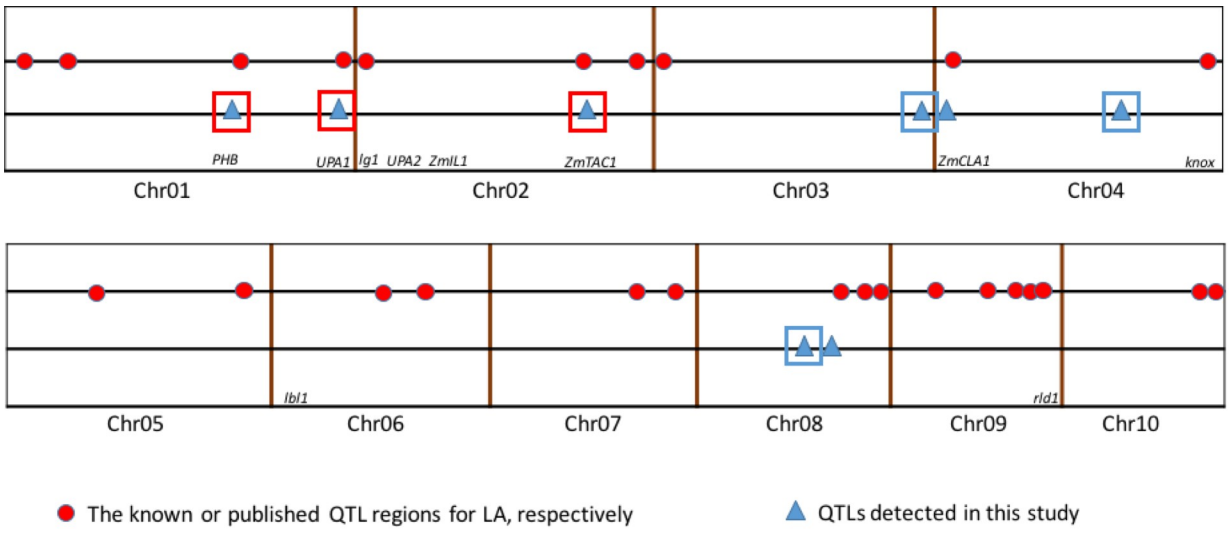

Fig 3. Comparison of QTL mapping results in this study with the results reported by previous researchers.

https://doi.org/10.1371/journal.pone.0245129.g003

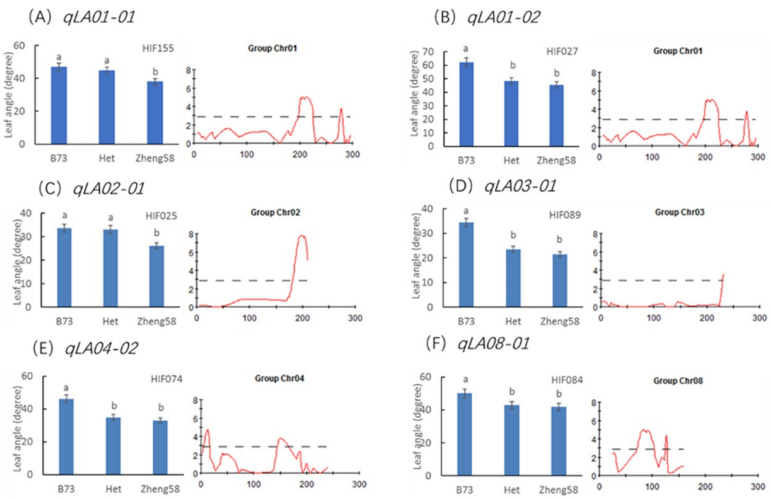

Fig 4. Significant analysis of the mean values of different genotypes in the same HIF population. The same letter indicates no significant difference between them, and different letters indicate a significant difference (P value < 0.05).

https://doi.org/10.1371/journal.pone.0245129.g004

Confirmation of QTL for leaf angle. There were some heterozygous regions in the genome of the F_4 plants. These regions can be applied to validation of QTL through a HIF strategy as described by Tuinstra et al. in 1997 [30]. The HIF strategy has been widely practiced in QTL confirmation and fine mapping [34,35]. In this study, we tried to apply the HIF strategy to validate the allelic effects of six major QTL for leaf angle. HIF segregating for the target QTL to be validated but homozygous for other major QTL regions were chosen. For instance, a RIL (HIF155) with heterozygous region in qLA01-01 was chosen to develop HIF. Theoretically, the leaf angle trait in progenies from selfed HIF155 will be only segregated for qLA01-01. We developed the other five HIFs in the same way. HIF027, HIF025, HIF089, HIF074 and HIF084 were heterozygous at marker umc1421 (qLA01-02), bnlg2077 (qLA02-01), bnlg1496 (qLA03-01), umc0371 (qLA04-02) and umc2147 (qLA08-01), respectively. The overview result for all HIF was presented in Fig 4. In the progenies of all HIFs, the plants carrying B73 alleles at the respective target QTL displayed a significantly bigger leaf angle than those carrying Zheng58 alleles. Therefore, the allelic effects of the major QTL were preliminarily validated.

Considering that the phenotype of leaf angle was easily affected by environmental conditions, we planted these 165 lines in the same season and the same field in 2014 and 2015. These 165 lines showed good repeatability in the phenotype of leaf angle and the phenotypic data were used to detected the QTL for leaf angle. The environmental factors affecting leaf angle phenotype were minimized and the QTL X environment effect was not detected. Subsequently, we construct the HIF populations to verify the major QTL, each HIF population with at least 120 plants. These plants were also grown in the same season and the same field in 2016. The results verified the authenticity of the QTL mapping results and showed that these major QTL are stable and inheritable. In this work, the character of the leaf angle trait resulted from the genetic characteristics of selected parents, Zheng58 and B73.

Whole-genome re-sequencing. In order to compare the genomic sequence differences between the two parents and predicted candidate genes for target QTL, Zheng58 was conducted the whole-genome re-sequencing. After filtering, 91.69 G bp Clean-Base was obtained for subsequent data analysis and the Q30 ratio reached 92.93%, with the 91.68% (at least one base coverage) genome coverage (S2 Table). By aligning against the B73 reference genome, the genome coverage on average for the reference up to 98.83%, which can give 37× average

genome sequencing coverage depth (S1 and S2 Figs). It can be seen from the figure (S2 Fig) that the genome is covered more uniformly, indicating that the sequencing randomness is better. The uneven depth on the map may be due to repeated sequences and PCR preferences. These data demonstrated that the whole-genome re-sequencing data was robust and can be used to subsequent candidate genes analysis.

Candidate genes prediction in major QTL qLA02-01 region. Comparing the genomic sequence differences in the qLA02-01 region between the two parents, we found that 156 genes were variated in the coding region, of which 18 stop gained SNP and 8 start lost SNP were related to 30 genes and 254 InDel (including 6 stop gained InDel, 2 start lost InDel and 246 frame-shift InDel) were related to 126 genes. Absolutely, stop gained and start lost, as well as frame-shift mutations often have a greater impact on causing changes in gene function. Thence, these mutations stimulated our further research interest. Although the mechanism underlying leaf angle is still unclear, previous studies have shown that genes associated with cell cycle, cell size, gravity and plant hormones may participate in regulation of leaf angle development [36]. By analysis of biological processes in the GO annotation clustering results, combined KEGG metabolic pathway analysis, we screened 33 GO enriched genes in the major qLA02-01 region (Table 3). With the help of GO term and functional annotation of candidate genes, ultimately six candidate genes are targeted: *Zm00001d005803*, auxin-activated signaling pathway (GO:0009734); *Zm00001d005888*, response to abscisic acid (GO:0009737); *Zm00001d005889*, oxidation-reduction process (GO:0055114); *Zm00001d006274*, auxin-activated signaling pathway (GO:0009734); *Zm00001d006494*, response to karrikin (GO:0080167); *Zm00001d006587*, response to blue light (GO:0009637).

In addition, variations in gene expression levels may also cause changes in gene function. Therefore, we also screened for genes with mutations in the promoter region, and 21 genes showed GO enrichment (Table 4). By analyzing the gene expression level of genes with mutations in the promoter region, we identified seven genes with significantly different expression levels (Fig 5): *Zm00001d005803*, auxin-activated signaling pathway (GO:0009734); *Zm00001d005818*, response to desiccation (GO:0009269); *Zm00001d005823*, oxidation-reduction process (GO:0055114); *Zm00001d005889*, oxidation-reduction process (GO:0055114); *Zm00001d006296*, regulation of translational fidelity (GO:0006450); *Zm00001d006443*, sister chromatid cohesion (GO:0007062); *Zm00001d006494*, response to karrikin (GO:0080167).

A total of 10 candidate genes were selected based on the structural variation of the gene promoter region and CDS region. There are three genes that have both genetic structure variation and promoter region variation: *Zm00001d005803*, *Zm00001d005889*, and *Zm00001d006494*. Thus, we suggest that *Zm00001d005803*, *Zm00001d005818*, *Zm00001d005823*, *Zm00001d005888*, *Zm00001d005889*, *Zm00001d006274*, *Zm00001d006296*, *Zm00001d006443*, *Zm00001d006494* and *Zm00001d006587* may be important candidate genes for qLA02-01.

Candidate genes prediction in major QTL qLA08-01 region

We found that 29 genes were variated in the coding region, by comparing the genomic sequence differences in the qLA08-01 region between the two parents, of which 18 stop gained SNP, 1 start lost SNP were related to 14 genes. What's more, 25 InDel were detected, including 1 start lost InDel, 1 stop lost InDel and 23 frame_shift InDel, related to 18 genes. Three of those 18 genes were displayed in SNP mutation as well.

12 GO enriched genes were screened in the major qLA08-01 region (Table 5), by analysis of biological processes in the GO annotation clustering results, combined KEGG metabolic pathway analysis. Besides, based on the promoter region mutation in Table 6 and 2 genes out of 17 shown significantly variations in gene expression levels (Fig 6).

Table 3. Selected candidate genes of leaf angle in qLA02-01 with mutations in the CDS region.

Gene ID	GO term	Description	Codon change	Effect
Zm00001d005614	oxidation-reduction process (GO:0055114);	Bifunctional protein FolD 1 mitochondrial	tga/	FRAME_SHIFT
Zm00001d005682	glucuronoxylan metabolic process (GO:0010413);	Protein kinase superfamily protein	atc/	FRAME_SHIFT
Zm00001d005785	isopentenyl diphosphate biosynthetic process, methylerythritol 4-phosphate pathway (GO:0019288);	Pentatricopeptide repeat-containing protein	att/aTtt	FRAME_SHIFT
Zm00001d005779	Biological Process: regulation of transcription, DNA-templated (GO:0006355);	ubiquitin carrier protein 7	Gga/Tga	STOP_GAINED
Zm00001d005792	negative regulation of catalytic activity (GO:0043086);	amidase1	gag/	FRAME_SHIFT
Zm00001d005803	auxin-activated signaling pathway (GO:0009734);	SAUR-like auxin-responsive protein family	gcc/gcGGc	FRAME_SHIFT
Zm00001d005808	phosphorylation (GO:0016310);	Probable ethanolamine kinase	cgt/cgTt	FRAME_SHIFT
Zm00001d005812	sister chromatid cohesion (GO:0007062);	sterile alpha motif (SAM) domain-containing protein	tta/ttTa	FRAME_SHIFT
Zm00001d005866	cell redox homeostasis (GO:0045454);	Protein disulfide-isomerase like 2–2	ttg/ttTTg	FRAME_SHIFT
Zm00001d005888	response to abscisic acid (GO:0009737);	Heat stress transcription factor B-3	taa/	FRAME_SHIFT
Zm00001d005889	oxidation-reduction process (GO:0055114);	abscisic acid 8'-hydroxylase 5	tgccgg/aca/	FRAME_SHIFT
Zm00001d005908	response to wounding (GO:0009611);	Tyrosine-sulfated glycopeptide receptor 1	ttt/ttGt	FRAME_SHIFT
Zm00001d005925	starch biosynthetic process (GO:0019252);	Glucose-6-phosphate isomerase 1 chloroplastic	gtt/	FRAME_SHIFT
Zm00001d005932	oxidation-reduction process (GO:0055114);	Aldose reductase	acg/aAcg	FRAME_SHIFT
Zm00001d006027	regulation of transcription, DNA-templated (GO:0006355);	bZIP transcription factor family protein	gct/tatgac/tcc/tccTCCGTCC	FRAME_SHIFT
Zm00001d006153	defense response by callose deposition (GO:0052542);	1-acylglycerol-3-phosphate O-acyltransferase	cca/	FRAME_SHIFT
Zm00001d006172	Biological Process: protein phosphorylation (GO:0006468);	Serine/threonine-protein kinase Rio1	tGg/tAg	STOP_GAINED
Zm00001d006193	oxidation-reduction process (GO:0055114);	cytochrome P450 family 78 subfamily A polypeptide 8	gcc/	FRAME_SHIFT
Zm00001d006274	auxin-activated signaling pathway (GO:0009734);	Auxin-responsive protein SAUR61	ggt/gAgt	FRAME_SHIFT
Zm00001d006295	protein phosphorylation (GO:0006468);	DNA-binding bromodomain-containing protein	ttg/ttgCTTGTTG	FRAME_SHIFT
Zm00001d006344	regulation of transcription, DNA-templated (GO:0006355);	Protein SUPPRESSOR OF FRI 4	ggt/ggGt	FRAME_SHIFT
Zm00001d006389	membrane fusion (GO:0006944);	small G protein family protein / RhoGAP family protein	ttt/att/	FRAME_SHIFT
Zm00001d006437	Biological Process: cell redox homeostasis (GO:0045454);	Monothiol glutaredoxin-S17	atG/atA	START_LOST
Zm00001d006476	glycolytic process (GO:0006096);	aconitase5	cct/ccTt	FRAME_SHIFT
Zm00001d006494	response to karrikin (GO:0080167);	Protein DETOXIFICATION 40	gcttttcctctctttttttttccc/aag/ aAGGTagatt/aTttctt/ttc/ttCCCCc	FRAME_SHIFT
Zm00001d006536	Biological Process: phosphorylation (GO:0016310);	Cysteine-rich receptor-like protein kinase 10	Gaa/Taa	STOP_GAINED
Zm00001d006548	response to wounding (GO:0009611);	Histone H2A	ctgctt/	FRAME_SHIFT
Zm00001d006586	response to salt stress (GO:0009651);	Peptidyl-prolyl cis-trans isomerase Pin1	tcccgcccgcagctc/	FRAME_SHIFT
Zm00001d006587	response to blue light (GO:0009637);	Chlorophyll a-b binding protein CP29.1 chloroplastic	atg/aAtg	FRAME_SHIFT
Zm00001d006622	Biological Process: electron transport chain (GO:0022900);	CYP72A57	Cag/Tag	STOP_GAINED

(*Continued*)

Table 3. (Continued)

Gene ID	GO term	Description	Codon change	Effect
Zm00001d006644	Biological Process: circadian rhythm (GO:0007623);	MAP kinase kinase kinase27	tgA/tgG	STOP_LOST
Zm00001d006675	DNA repair (GO:0006281);	ATP-dependent DNA helicase	gtt/gTtt	FRAME_SHIFT
Zm00001d006681	negative regulation of transcription, DNA-templated (GO:0045892);	unknown	atg/	START_LOST

https://doi.org/10.1371/journal.pone.0245129.t003

In all, 14 candidate genes were filtered as candidate gene. And the result indicates that *Zm00001d009622* (Biological Process: transcription, DNA-templated (GO:0006351)), *Zm00001d009642* (Biological Process: membrane fusion (GO:0006944)), *Zm00001d009671* (Biological Process: potassium ion transmembrane transport (GO:0071805)), *Zm00001d009676* (Biological Process: protein phosphorylation (GO:0006468)), *Zm00001d009730* (Biological Process: translation (GO:0006412)), *Zm00001d009737* (Biological Process: GTP catabolic process (GO:0006184)), *Zm00001d009754* (Biological Process: cell wall macromolecule catabolic process (GO:0016998)), *Zm00001d009789* (Biological Process: borate transport (GO:0046713)), *Zm00001d009802*(Biological Process: protein transport (GO:0015031)), *Zm00001d009871* (Biological Process: transmembrane transport (GO:0055085); Biological Process: GDP-mannose transport (GO:0015784)), *Zm00001d009948*(Biological Process: response to heat (GO:0009408)), *Zm00001d009962* (Biological Process: protein import into nucleus (GO:0006606)), *Zm00001d009610* (Acetamidase / Formamidase family protein), *Zm00001d009835* (Triosephosphate isomerase cytosolic) may be important candidate genes for qLA08-01.

Table 4. Selected candidate genes of leaf angle in qLA02-01 with mutations in the promoter region.

Gene ID	GO term	Description	Effect
Zm00001d005682	glucuronoxylan metabolic process (GO:0010413);	Protein kinase superfamily protein	UPSTREAM
Zm00001d005803	auxin-activated signaling pathway (GO:0009734);	SAUR-like auxin-responsive protein family	UPSTREAM
Zm00001d005808	phosphorylation (GO:0016310);	Probable ethanolamine kinase	UPSTREAM
Zm00001d005818	response to desiccation (GO:0009269);	Aldehyde dehydrogenase family 7 member B4	UPSTREAM
Zm00001d005823	oxidation-reduction process (GO:0055114);	Flavonoid 3-monooxygenase	UPSTREAM
Zm00001d005888	endoplasmic reticulum unfolded protein response (GO:0030968);	Heat stress transcription factor B-3	UPSTREAM
Zm00001d005889	oxidation-reduction process (GO:0055114);	abscisic acid 8'-hydroxylase5	UPSTREAM
Zm00001d006027	endoplasmic reticulum unfolded protein response (GO:0030968);	bZIP transcription factor family protein	UPSTREAM
Zm00001d006036	response to salt stress (GO:0009651);	Heat shock 70 kDa protein 9 mitochondrial	UPSTREAM
Zm00001d006153	toxin catabolic process (GO:0009407);	1-acylglycerol-3-phosphate O-acyltransferase	UPSTREAM
Zm00001d006285	auxin-activated signaling pathway (GO:0009734);	SAUR52-auxin-responsive SAUR family member	UPSTREAM
Zm00001d006296	regulation of translational fidelity (GO:0006450);	Valine—tRNA ligase mitochondrial 1	UPSTREAM
Zm00001d006389	membrane fusion (GO:0006944);	small G protein family protein / RhoGAP family protein	UPSTREAM
Zm00001d006443	sister chromatid cohesion (GO:0007062);	P-loop containing nucleoside triphosphate hydrolases superfamily protein	UPSTREAM
Zm00001d006467	cysteine biosynthetic process (GO:0019344);	adenosine 5'-phosphosulfate reductase-like2	UPSTREAM
Zm00001d006494	response to karrikin (GO:0080167);	Protein DETOXIFICATION 40	UPSTREAM
Zm00001d006629	protein phosphorylation (GO:0006468);	Mitochondrial transcription termination factor family protein	UPSTREAM
Zm00001d006631	transmembrane transport (GO:0055085);	Organic cation/carnitine transporter 7	UPSTREAM
Zm00001d006646	phosphorylation (GO:0016310);	unknown	UPSTREAM
Zm00001d006688	transmembrane transport (GO:0055085);	Putative polyol transporter 1	UPSTREAM
Zm00001d006700	root development (GO:0048364);	mTERF family protein	UPSTREAM

https://doi.org/10.1371/journal.pone.0245129.t004

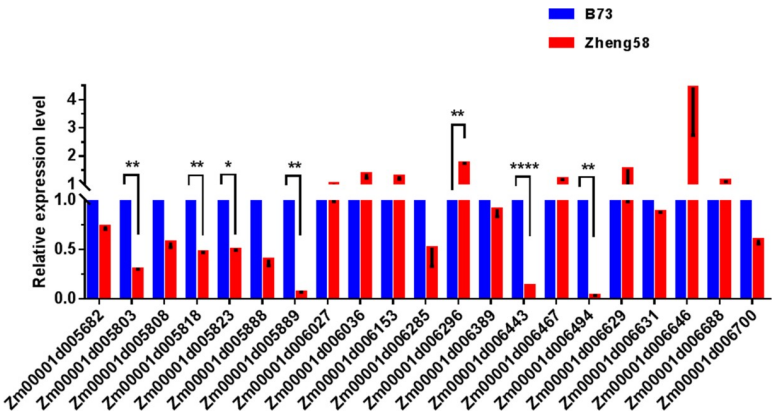

Fig 5. The expression levels of the candidate genes on qLA02-01 loci in the two parents, B73 and Zheng58. The expression level of each candidate gene in B73 is set to 1. The data is the mean ± SD (n = 3). P<0.05 (Student's t-test).

https://doi.org/10.1371/journal.pone.0245129.g005

Conclusion

In conclusion, the study of genetic basis of leaf angle is important for maize breeding. In the study, eight QTL for leaf angle were detected and most QTL were validated through HIF

Table 5. Selected candidate genes of leaf angle in qLA08-01 with mutations in the CDS region.

Gene ID	GO term	Description	Codon change	Effect
Zm00001d009622	Biological Process: transcription, DNA-templated (GO:0006351);	Putative AP2/EREBP transcription factor superfamily protein	atc/ atcGGCGCCCGCATGACGCGGAAGCGCGgct/ tcc/tccTatg/	FRAME_SHIFT FRAME_SHIFT FRAME_SHIFT START_LOST
Zm00001d009642	Biological Process: membrane fusion (GO:0006944);	F-box protein	cta/	FRAME_SHIFT
Zm00001d009671	Biological Process: potassium ion transmembrane transport (GO:0071805);	Potassium transporter 10	tGg/tAg	STOP_GAINED
Zm00001d009676	Biological Process: protein phosphorylation (GO:0006468);	serine/threonine protein kinase 3	gac/gaCctcggac/	FRAME_SHIFT
Zm00001d009730	Biological Process: translation (GO:0006412);	unknown	aaa/	FRAME_SHIFT
Zm00001d009737	Biological Process: GTP catabolic process (GO:0006184);	Tubulin beta-2 chain	Cag/Tag	STOP_GAINED
Zm00001d009754	Biological Process: cell wall macromolecule catabolic process (GO:0016998);	unknown	tac/	FRAME_SHIFT
Zm00001d009789	Biological Process: borate transport (GO:0046713);	Boron transporter 4	agg/	FRAME_SHIFT
Zm00001d009802	Biological Process: protein transport (GO:0015031);	Putative homeobox DNA-binding and leucine zipper domain family protein	cta/cCCta	FRAME_SHIFT
Zm00001d009871	Biological Process: transmembrane transport (GO:0055085); Biological Process: GDP-mannose transport (GO:0015784);	GDP-mannose transporter GONST1	gga/	FRAME_SHIFT
Zm00001d009948	Biological Process: response to heat (GO:0009408);	Heat shock 70 kDa protein 14	cgagga/	FRAME_SHIFT
Zm00001d009962	Biological Process: protein import into nucleus (GO:0006606);	Sas10/Utp3/C1D family	gtt/gGtt	FRAME_SHIFT

https://doi.org/10.1371/journal.pone.0245129.t005

Table 6. Selected candidate genes of leaf angle in qLA08-01 with mutations in the promoter region.

Gene ID	GO term	Description	Effect
Zm00001d009580		Urease accessory protein G	UPSTREAM
Zm00001d009593		unknown	UPSTREAM
Zm00001d009594		Aspartic proteinase A1	UPSTREAM
Zm00001d009610		Acetamidase/Formamidase family protein	UPSTREAM
Zm00001d009611		unknown	UPSTREAM
Zm00001d009612		DUF1645 family protein	UPSTREAM
Zm00001d009619		Putative WRKY DNA-binding domain superfamily protein	UPSTREAM
Zm00001d009620		Probable protein phosphatase 2C 33	UPSTREAM
Zm00001d009622	Biological Process: transcription, DNA-templated (GO:0006351);	Putative AP2/EREBP transcription factor superfamily protein	UPSTREAM
Zm00001d009631		CTP synthase family protein	UPSTREAM
Zm00001d009679		ATP-dependent DNA helicase	UPSTREAM
Zm00001d009704			UPSTREAM
Zm00001d009813		Nucleotide/sugar transporter family protein	UPSTREAM
Zm00001d009835		Triosephosphate isomerase cytosolic	UPSTREAM
Zm00001d010000		Thioredoxin-like 2–2 chloroplastic	UPSTREAM
Zm00001d010009	Biological Process: translation (GO:0006412);	ribosomal protein L17a	UPSTREAM
Zm00001d010152		Histone deacetylase 8	UPSTREAM

https://doi.org/10.1371/journal.pone.0245129.t006

approach. Candidate gene analysis within the qLA02-01 and qLA08-01 regions was conducted by whole-genome re-sequencing and expression analysis and twenty-four candidate genes for leaf angle were predicted. This study provides a better understanding of the genetic basis of leaf angle. To validate the functionality of candidate genes, future studies should be conducted using RNA-seq at the key developmental stage of maize leaf angle formation. This should alleviate inaccuracies due to differences in DNA sequences between the two parents. Furthermore, moderate fine mapping is more operable to eliminate the blindness of the authentic gene identification. Techniques such as gene editing could be utilized to edit the allele of our candidate genes, which could identify the authentic genes for qLA02-01 and qLA08-01. The cloning and function research of genes in qLA02-01 and qLA08-01 would improve our knowledge about plant architecture, and also can supply good candidate genes for molecular breeding of crops.

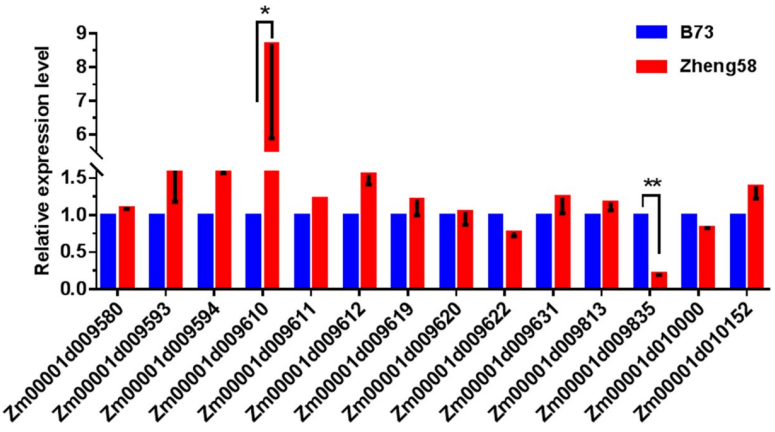

Fig 6. The expression levels of the candidate gene on qLA08-01 loci in the two parents., B73 and Zheng58. The expression level of each candidate gene in B73 is set to 1. The data is the mean ± SD (n = 3). P<0.05 (Student's t-test).

https://doi.org/10.1371/journal.pone.0245129.g006

Supporting information

S1 Fig. The basic situation of the sequencing depth distribution.
(DOCX)

S2 Fig. Genome wide distribution of read coverage. The horizontal axis is the chromosomal position, and the vertical axis is the median of read density of the corresponding position on the chromosome (log (2)). There is no significant difference at the 5% level. Error bars indicate the standard deviation of the phenotypic values for each genotype.
(DOCX)

S1 Table. RT-qPCR primer.
(DOCX)

S2 Table. Whole genome resequencing results of Zheng58.
(DOCX)

Acknowledgments

The authors are grateful to Institute of Crop Science, Chinese Academy of Agricultural Sciences (ICS, CAAS) and Chinese Crop Germplasm Resources Information System (CGRIS) for providing seeds of the maize inbred lines for experiment. We thank the BioMarker Technologies Company for providing sequencing services.

Author Contributions

Conceptualization: Ning Zhang.

Formal analysis: Ning Zhang.

Investigation: Ning Zhang.

Software: Ning Zhang.

Writing – original draft: Ning Zhang, Xueqing Huang.

Writing – review & editing: Ning Zhang, Xueqing Huang.

References

1. Duvick DN, Smith JSC, Cooper M. Long-term selection in a commercial hybrid maize breeding program. Plant Breed Rev. 2017; 24: 109–151.
2. Duncan WG. Leaf angles, leaf area, and canopy photosynthesis1. Crop Sci. 1971; 11: 482–485.
3. Lambert RJ, Johnson RR. Leaf angle, tassel morphology, and the performance of maize hybrids. Crop Sci. 1978; 18:499–502.
4. Pepper GE, Pearce RB, Mock JJ. Leaf orientation and yield of maize. Crop Sci. 1977; 17: 883–886.
5. Pendleton JW, Smith GE, Winter SR, Johnston TJ. Field investigations of the relationships of leaf angle in corn (Zea mays L.) to grain yield and apparent photosynthesis. Agron J. 1968; 60(4): 422–424.
6. Duvick DN. The contribution of breeding to yield advances in maize (Zea mays L.). Adv Agron. 2005; 86: 83–145.
7. Schneeberger RG, Becraft PW, Hake S, Freeling M. Ectopic expression of the knox homeo box gene rough sheath1 alters cell fate in the maize leaf. Genes Dev. 1995; 9(18): 2292–2304. https://doi.org/10.1101/gad.9.18.2292 PMID: 7557382
8. Moreno MA, Harper LC, Krueger RW, Dellaporta SL, Freeling M. Liguleless1 encodes a nuclear-localized protein required for induction of ligules and auricles during maize leaf organogenesis. Genes Dev. 1997; 11: 616–628. https://doi.org/10.1101/gad.11.5.616 PMID: 9119226

9. Walsh J, Waters CA, Freeling M. The maize gene liguleless2 encodes a basic leucine zipper protein involved in the establishment of the leaf blade-sheath boundary. Genes Dev. 1998; 12(2): 208–218. https://doi.org/10.1101/gad.12.2.208 PMID: 9490265

10. Muehlbauer GJ, Fowler JE, Freeling M. Sectors expressing the homeobox gene liguleless3 implicate a time-dependent mechanism for cell fate acquisition along the proximal-distal axis of the maize leaf. Development. 1997; 124(24): 5097–5106. PMID: 9362467

11. Moon J, Candela H, Hake S. The Liguleless narrow mutation affects proximal-distal signaling and leaf growth. 2013; 140(2): 405–412. https://doi.org/10.1242/dev.085787 PMID: 23250214

12. Ku LX, Wei XM, Zhang SF, Zhang J, Guo SL, Chen YH. Cloning and Characterization of a Putative TAC1 Ortholog Associated with Leaf Angle in Maize (Zea mays L.). PLoS ONE. 2011; 6(6): e20621. https://doi.org/10.1371/journal.pone.0020621 PMID: 21687735

13. Zhang J, Ku LX, Han ZP, Guo SL, Liu HJ, Zhang ZZ, et al. The ZmCLA4 gene in the qLA4-1 QTL controls leaf angle in maize (Zea mays L.). J. Exp. Bot. 2014; 65(17): 5063–5076. https://doi.org/10.1093/jxb/eru271 PMID: 24987012

14. Ren ZZ, Wu LC, Ku LX, Wang HT, Zeng HX, Su HH, et al. ZmILI1 regulates leaf angle by directly affecting liguleless1 expression in maize. Plant Biotechnol. J. 2020; 18(4): 881–883. https://doi.org/10.1111/pbi.13255 PMID: 31529573

15. Tian JG, Wang CL, Xia JL, Wu LS, Xu GH, Wu WH, et al. Teosinte ligule allele narrows plant architecture and enhances high-density maize yields. Science. 2019; 365(6454): 658–664. https://doi.org/10.1126/science.aax5482 PMID: 31416957

16. Gao YY, Zeng H, Ku LX, Ren ZZ, Han Y, Su HH, et al. ZmIBH1-1 regulates plant architecture in maize. J Exp Bot. 2020; 71(10): 2943–2955. https://doi.org/10.1093/jxb/eraa052 PMID: 31990030

17. Mickelson SM, Stuber CS, Senior L, Kaepple SM. Quantitative trait loci controlling leaf and tassel traits in a B73×Mo17 population of maize. Crop Sci. 2002; 42(6): 1902–1909.

18. Yu YT, Zhang JM, Shi YS, Song YC, Wang TY, Li Y. QTL analysis for plant height and leaf angle by using different populations of maize. Maize Sci. 2006; 14(2): 88–92.

19. Ku LX, Zhao WM, Zhang J, Wu LC, Wang CL, Wang PA, et al. Quantitative trait loci mapping of leaf angle and leaf orientation value in maize (Zea mays L.). Theor Appl Genet. 2010; 121(5): 951–959. https://doi.org/10.1007/s00122-010-1364-z PMID: 20526576

20. Lu M, Zhou F, Xie CX, Li MS, Xu YB, Marilyn W, et al. Construction of a SSR linkage map and mapping of quantitative trait loci (QTL) for leaf angle and leaf orientation with an elite maize hybrid. Hereditas. 2007; 29(9): 1131–1138. https://doi.org/10.1360/yc-007-1131 PMID: 17855265

21. Ku LX, Zhang J, Guo SL, Liu HY, Zhao RF,Chen YH. Integrated multiple population analysis of leaf architecture traits in maize (Zea mays L.). J Exp Bot. 2012; 63(1): 261–274. https://doi.org/10.1093/jxb/err277 PMID: 21984652

22. Chen XN, Xu D, Liu Z, Yu TT, Mei XP, Cai YL. Identification of QTL for leaf angle and leaf space above ear position across different environments and generations in maize (Zea mays L.). Euphytica. 2015; 204: 395–405.

23. Li C, Li Y, Shi Y, Song Y, Zhang D, Buckler ES, et al. Genetic Control of the Leaf Angle and Leaf Orientation Value as Revealed by Ultra-High Density Maps in Three Connected Maize Populations. PLoS ONE. 2015; 10(3): e0121624. https://doi.org/10.1371/journal.pone.0121624 PMID: 25807369

24. Dzievit MJ, Li X, Yu J. Dissection of Leaf Angle Variation in Maize through Genetic Mapping and Meta-Analysis. Plant Genome. 2019; 12(1). https://doi.org/10.3835/plantgenome2018.05.0024 PMID: 30951086

25. Lu S, Zhang M, Zhang Z, Wang Z, Wu N, Song Y, et al. Screening and verification of genes associated with leaf angle and leaf orientationvalue in inbred maize lines. PLoS One. 2018; 13(12): e0208386. https://doi.org/10.1371/journal.pone.0208386 PMID: 30532152

26. Tian F, Bradbury PJ, Brown PJ, Hung H, Sun Q, Flint-Garcia S, et al. Genome-wide association study of leaf architecture in the maize nested association mapping population. Nat Genet. 2011; 43(2): 159–162. https://doi.org/10.1038/ng.746 PMID: 21217756

27. Ding JQ, Zhang LY, Chen JF, Li XT, Li YM, Cheng HL, et al. Genomic dissection of leaf angle in Maize (Zea mays L.) using a four-way cross mapping population. PLoS ONE. 2015; 10(10): e0141619. https://doi.org/10.1371/journal.pone.0141619 PMID: 26509792

28. Lai JS, Li RQ, Xu X, Jin WW, Xu ML, Zhao HN, et al. Genome-wide patterns of genetic variation among elite maize inbred lines. Nat Genet. 2010; 42(11): 1027–1030. https://doi.org/10.1038/ng.684 PMID: 20972441

29. Yang Z, Li X, Zhang N, Wang XL, Zhang YN, Ding YL, et al. Mapping and validation of the quantitative trait loci for leaf stay-green-associated parameters in maize. Plant Breeding. 2017; 136(2): 188–196.

30. Tuinstra MR, Ejeta G, Goldsbrough PB. Heterogeneous inbred family (HIF) analysis: a method for developing near-isogenic lines that differ at quantitative trait loci. Theor Appl Genet. 1997; 95(5): 1005–1011.

31. Murray MG, Thompson WF. Rapid isolation of high weight plant DNA. Nucleic Acids Res. 1980; 8: 4321–4325. https://doi.org/10.1093/nar/8.19.4321 PMID: 7433111

32. Churchill GA, Doerge RW. Empirical threshold values for quantitative trait mapping. Genetics. 1994; 138(3): 963–971. PMID: 7851788

33. Huang XQ, Schmitt J, Dorn L, Griffith C, Effgen S, Takao S, et al. The earliest stages of adaptation in an experimental plant population: strong selection on QTLS for seed dormancy. Mol Ecol. 2010; 19(7): 1335–1351. https://doi.org/10.1111/j.1365-294X.2010.04557.x PMID: 20149097

34. Jimenez-Gomez JM, Wallace AD, Maloof JN. Network Analysis Identifies ELF3 as a QTL for the shade avoidance response in Arabidopsis. PLoS Genet. 2010; 6(9): e1001100. https://doi.org/10.1371/journal.pgen.1001100 PMID: 20838594

35. Liu Y, Zhu XY, Zhang S, Bernardo M, Edwards J, Galbraith DW, et al. Dissecting quantitative resistance against blast disease using heterogeneous inbred family lines in rice. Theor Appl Genet. 2011; 122(2): 341–353. https://doi.org/10.1007/s00122-010-1450-2 PMID: 20872132

36. Wang YH, Li JY. Molecular basis of plant architecture. Annu Rev Plant Biol. 2008; 59: 253–279. https://doi.org/10.1146/annurev.arplant.59.032607.092902 PMID: 18444901